NUCL SCI TECH (2017) 28:182
https://doi.org/10.1007/s41365-017-0337-1

# Electromagnetic field effects on nucleon transverse momentum for heavy ion collisions around 100 A MeV

Xian-Gai Deng[1,2] · Yu-Gang Ma[1,3]

Received: 12 October 2017 / Revised: 2 November 2017 / Accepted: 4 November 2017 / Published online: 22 November 2017


**Abstract** With taking electromagnetic field into account for the transport model of Boltzmann-Uehling-Uhlenbeck, electromagnetic effects are studied for $^{208}$Pb $+ ^{208}$ Pb collisions around 100*A* MeV. Electromagnetic field evolution during the collisions was estimated. It was found that the electric field has an obvious effect on the transverse momentum ($p_T$) spectra of nucleons during heavy ion collisions, and leads to different minimum position for the peak of $p_T$ spectra of nucleons versus beam energy when the electric field is switched on. For the magnetic field, it affects the *z*-axis direction distributions of nucleons for central heavy ion collisions at lower energy.

**Keywords** Heavy ion collision · Electromagnetic field · Transverse momentum

*Dedicated to Joseph B. Natowitz in honour of his 80th birthday.*

This work was supported by the National Natural Science Foundation of China (Nos. 11421505, 11305239, and 11220101005), the Major State Basic Research Development Program in China (No. 2014CB845401), the Key Research Program of Frontier Sciences of CAS (No. QYZDJSSW-SLH002), and the Strategic Priority Research Program of the Chinese Academy of Sciences (No. XDB16).

✉ Yu-Gang Ma
ygma@sinap.ac.cn

1 Shanghai Institute of Applied Physics, Chinese Academy of Sciences, Shanghai 201800, China

2 University of Chinese Academy of Sciences, Beijing 100049, China

3 ShanghaiTech University, Shanghai 200031, China

## 1 Introduction

In heavy ion collisions, strong electrical fields and magnetic fields should be considered which was firstly pointed out by the Rafelski and Müller in Ref. [1]. With our well knowledge, the Coulomb force causes the repulsive interactions for the charge particles and the Lorentz force can alter the velocities of charge particles. Many efforts have been paid for the Coulomb effects in heavy ion collisions [2–8]. The electric fields treated as static electric fields (Coulomb fields) have been taken into account in most transport models for the study of nuclear matter of intermediate energy heavy ion collisions. In Ref. [9], the electromagnetic fields are considered with the velocities of charge particles in heavy ion collisions at intermediate energies within the Boltzmann-Uehling-Uhlenbeck (BUU) transport model. The magnetic field created in noncentral Au + Au collision at $\sqrt{s} = 200$ GeV at the relativistic heavy ion collider (RHIC) can reach about $eB \sim m_\pi^2 \sim 10^{18}$ Gauss (in Lorentz units, $1\ \mathrm{MeV}^2 \approx 5.11 \times 10^{13}$ Gauss) [9–13]. Experimental and theoretical indications showed that the QCD topological effects such as the chiral magnetic effect (CME) in the intense electromagnetic fields may be the evidence of local parity violation in strong interactions [14–21]. The properties of strange quark matter in a strong external electric and magnetic field will be also significantly influenced [22–24]. Very recently, the strongest votical motion has been deduced from the polarization measurement of $\Lambda$ hyperon in Au + Au collisions at 200 GeV/*c* by the STAR collaboration [25] which is consistent with the prediction of the global polarization of the quark–gluon plasma [26].

But electromagnetic field, especially for the magnetic field, is seldom investigated at low energy for heavy ion collisions where is far from pion production energies. So the aim of this paper is to study the electromagnetic effects at low energies ranging from 40 to 120 MeV/nucleon for Pb + Pb heavy ion collisions.

The organization of the paper is as follows: In Sect. 2, we give a brief introduction of the simulation model including electromagnetic field. Results of electromagnetic field and electromagnetic field effects are discussed in Sect. 3.1. Finally, a summary is given in the end.

## 2 Theoretical framework

### 2.1 Boltzmann-Uehling-Uhlenbeck model

The BUU model is a very popular tool for describing intermediate energy heavy ion collision [27, 28], which is a one-body mean-field theory based upon the Boltzmann equation [29]. The BUU equation reads [30]

$$\begin{aligned}&\frac{\partial f}{\partial t}+\upsilon\nabla_r f-\nabla_r U\nabla_p f\\&=\frac{4}{(2\pi)^3}\int \mathrm{d}^3p_2\mathrm{d}^3p_3\mathrm{d}\Omega\frac{\mathrm{d}\sigma_{\mathrm{NN}}}{\mathrm{d}\Omega}\upsilon_{12}\times[f_3f_4(1-f)\\&\quad\times(1-f_2)-ff_2(1-f_3)(1-f_4)]\delta^3(p+p_2-p_3-p_4),\end{aligned}\tag{1}$$

where $f=f(\mathbf{r},\mathbf{p},t)$ is the phase-space distribution function. One can solve this equation by the method of Bertsch and Das Gupta [31]. In Eq. (1), $\frac{\mathrm{d}\sigma_{\mathrm{NN}}}{\mathrm{d}\Omega}$ and $\upsilon_{12}$ are nucleon–nucleon cross section and the relative velocity for the colliding nucleons, respectively. The nucleon–nucleon cross sections include the elastic and inelastic ones, and the well-known parametrization of Cugnon, Mizutani, and Vandermeulun [32] as a function of the available center-of-mass energy has been used. The details of the BUU model were described in Ref. [31].

And the mean-field potential $U$ including the isospin-dependent symmetry energy term can be given

$$U(\rho,\tau_z)=a\left(\frac{\rho}{\rho_0}\right)+b\left(\frac{\rho}{\rho_0}\right)^{\kappa}+C_{\mathrm{sym}}\left(\frac{\rho_{\mathrm{n}}-\rho_{\mathrm{p}}}{\rho_0}\right)\tau_z,\tag{2}$$

where $\rho_0(\rho_0=0.168\,\mathrm{fm}^{-3})$, $\rho_{\mathrm{n}}$, and $\rho_{\mathrm{p}}$ are the normal nuclear matter, neutron, and proton densities; and $\tau_z$ equals 1 or $-1$ for neutrons and protons, respectively; and $C_{\mathrm{sym}}$ is the coefficient of the symmetry energy term (here $C_{\mathrm{sym}}=32$ MeV is used). The coefficients $a$, $b$, and $\kappa$ are parameters for the nuclear equation of state (EoS). In this work, we use one set of mean-field parameters, the semi-soft EoS with the compressibility $K$ of 235 MeV ($a=-218$ MeV, $b=$ 164 MeV, $\kappa=4/3$).

One can appropriately implement the electrical and magnetic fields into transport model according to the Liénard–Wiechert potentials at a position $\vec{r}$ and time $t$ [9, 33]

$$e\vec{E}(\vec{r},t)=\frac{e^2}{4\pi\epsilon_0}\sum_n Z_n\frac{c^2-\upsilon_n^2}{(cR_n-\vec{R}_n\cdot\vec{\upsilon}_n)^3}(c\vec{R}_n-R_n\vec{\upsilon}_n),\tag{3}$$

$$e\vec{B}(\vec{r},t)=\frac{e^2}{4\pi\epsilon_0 c}\sum_n Z_n\frac{c^2-\upsilon_n^2}{(cR_n-\vec{R}_n\cdot\vec{\upsilon}_n)^3}\vec{\upsilon}_n\times\vec{R}_n,\tag{4}$$

where in the left-hand side, an additional charge $e$ is in order to get the electromagnetic fine structure constant $\alpha=e^2/4\pi=1/137$ (setting $\epsilon_0=\hbar=c=1$ ) in the right side of Eqs. (4) and (5). And $Z_n$ is the charge number of the $n$th particle; $\vec{R}_n=\vec{r}-\vec{r}'_n$, where $\vec{r}'_n$ is position of charge particle moving with the velocity $\vec{\upsilon}_n$ at retarded time $t_{rn}=t-|\vec{r}-\vec{r}'_n(t_{rn})|/c$. In nonrelativistic approximation, when $\upsilon\ll c$, one can obtain:

$$e\vec{E}(\vec{r},t)=\frac{e^2}{4\pi\epsilon_0}\sum_n Z_n\frac{1}{R_n^3}\vec{R}_n,\tag{5}$$

$$e\vec{B}(\vec{r},t)=\frac{e^2}{4\pi\epsilon_0 c}\sum_n Z_n\frac{1}{R_n^3}\vec{\upsilon}_n\times\vec{R}_n.\tag{6}$$

With adding the electrical and magnetic fields, the Hamilton's equations of propagations of nucleons become

$$\frac{\mathrm{d}\vec{p}_i}{\mathrm{d}t}=-\nabla_r U(\vec{r}_i)+\vec{F}_{\mathrm{C}}(\vec{r}_i)+\vec{F}_{\mathrm{L}}(\vec{r}_i),\tag{7}$$

$$\frac{\mathrm{d}\vec{r}_i}{\mathrm{d}t}=\frac{\vec{p}_i}{\sqrt{m^2+\vec{p}_i^2}},\tag{8}$$

where $\vec{F}_{\mathrm{C}}(\vec{r}_i)$ and $\vec{F}_{\mathrm{L}}(\vec{r}_i)$ are Coulomb and magnetic force of $i$th particle, respectively. We have to mention that for dealing with the initial distance of target and projectile, we did it as the same way which was mentioned in Ref. [9].

## 3 Results and discussion

### 3.1 Space-time evolution of the electromagnetic field

First we plot the time evolutions of nucleon density (top panels), electric field in the $z$ direction (middle panels), and magnetic field in the $y$ direction (bottom panels) in the $x$–$z$ plane at impact parameter of $b=0.5\times b_{\max}$ [$b_{\max}=1.12\times(A_{\mathrm{P}}^{1/3}+A_{\mathrm{T}}^{1/3})$] fm for the 40 MeV/nucleon $^{208}$Pb + $^{208}$Pb collisions in Fig. 1. The characteristics of electric fields (middle panels) in the $z$ direction display the geometric configurations of two collision nuclei as shown in top panels of Fig. 1. There are two parts in the zone of each nucleus for the electric field $eE_z$ at the early stage of reaction, as shown in Fig. 1b1, b2. At later stage, a

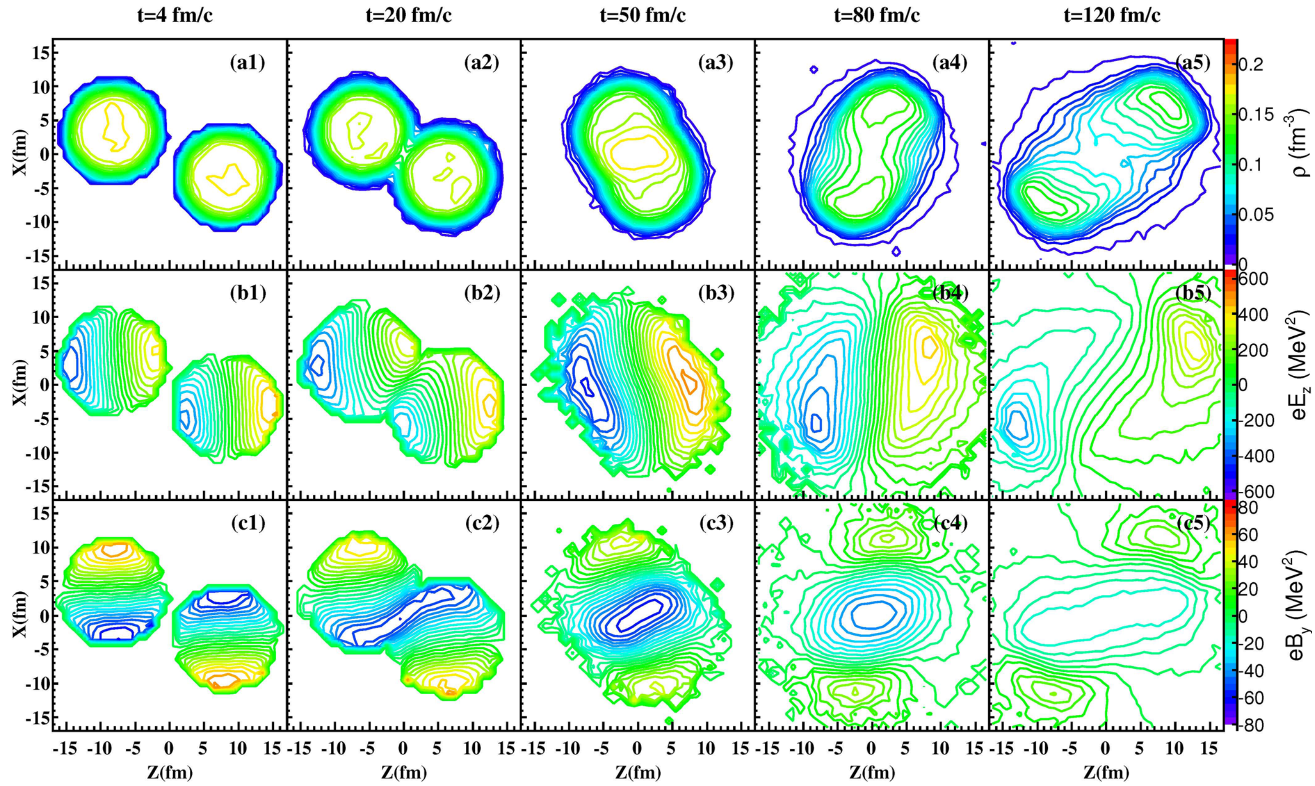


**Fig. 1** (Color online) Time evolutions of distributions of nucleons density $\rho$ (top), $x$-axis of electrical field $eE_x$ (middle), and $y$-axis of magnetic field $eB_y$ (bottom) in the $x$–$z$ plane at impact parameter of $b = 0.5 \times b_{\max}$ fm for the 40 MeV/nucleon $^{208}$Pb $+ ^{208}$Pb collisions

compound system occurs between nuclei and the shapes of nuclei influence the distribution of electric field which are formed two parts as shown in Fig. 1b3. As time increases, they maintain it except for the strength decreasing. The magnetic field $eB_y$ forms differently in comparison with electric field $eE_z$. The magnetic field forms a center and two spectator zones about 20 fm/$c$. When the reactions reach maximum compression, the center zone of magnetic field becomes smaller and strength becomes larger. Compared with the strength of electromagnetic field in relativistic heavy ion collisions [10], the strengths (electricfield $\approx 5 \times 10^{-3} m_\pi$ and magnetic field $\approx 5 \times 10^{-3} m_\pi$) are too small here. Our calculations for the distributions of nucleon density and electromagnetic field are similar to the calculation by Ou and Li [9].

In addition, we give the evolution of magnetic field in the $y$ direction at center position $R(0, 0, 0)$ at different impact parameters and incident energies in Figs. 2 and 3, respectively. The time evolution of average $eB_y(0,0,0)$ around zero for the central collision is shown in Fig. 2. The maximum values increase with the impact parameters for the situation of $b = 1.5 \times b_{\max}$ fm. It is due to different definition of initial position of target and projectile. In Fig. 3, the maximum values of the average $eB_y(0,0,0)$ increase with the beam energies. The strengths of

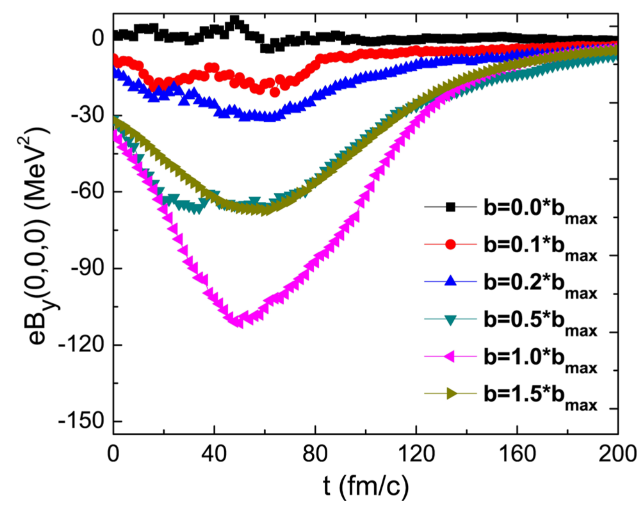


**Fig. 2** (Color online) Time evolution of $eB_y$(0,0,0) at different impact parameters for the 40 MeV/nucleon $^{208}$Pb $+ ^{208}$Pb collisions

$eB_y(0,0,0)$ are negative in Figs. (2) and (3) due to the relative position of target and projectile, as shown in the top of Fig. 1. It is more opposite than the results in Ref. [9].

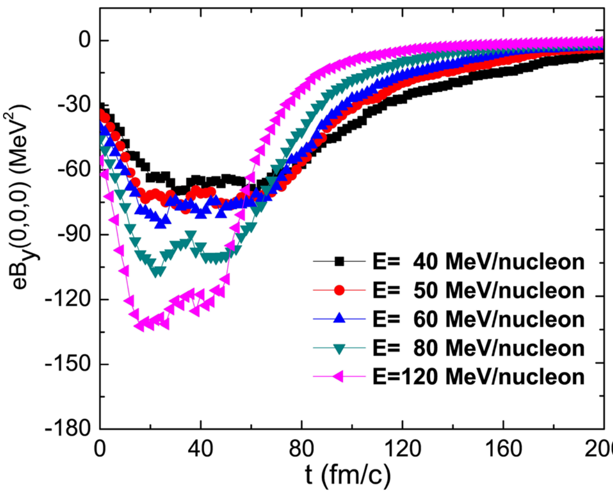


**Fig. 3** (Color online) Time evolution of $eB_y(0{,}0{,}0)$ at different beam energies for $^{208}$Pb $+^{208}$ Pb collisions at the impact parameter of $b = 0.5 \times b_{\max}$ fm

### 3.2 Electric effects on $p_{\mathrm{T}}$ spectra

One should be acquainted with Coulomb interaction for the EoS in heavy ion collisions. Coulomb effects on flows have been studied around the balance energy in many literatures, e.g., Refs. [8, 34, 35]. In our work, the electric field is included in the simulation model considering the velocities of charge particles in the reaction system. Here, electric effects are explored by $p_{\mathrm{T}}$ spectra of nucleons at beam energy of 40 MeV/nucleon and impact parameter of $b = 0$ fm, as shown in Fig. 4. It is worth to mention here that distributions of $p_{\mathrm{T}} (= \sqrt{p_x^2 + p_y^2})$ of nucleons will keep stable when the reactions reach freeze-out stage. And we extracted the distributions from the final stage of reactions in Fig. 4. It shows that $p_{\mathrm{T}}$ peak shifts to left when including electric field (with $E$), which indicates that the beam energy becomes difficult to convert into the transverse energy with the Coulomb interaction is included at 40 MeV/nucleon, which also makes the system hard thermalized at lower beam energy. Two peak values of the solid line (without $E$) and dash line (with $E$) are extracted by the fitting and shown in Fig. 4. Interestingly, a minimum value emerges from the dependence of peak values on beam energy as shown in Fig. 5a. From the square-blue line without $E$, the minimum value emerges around 80 MeV/nucleon. Also as the dot-red line shows, there is another minimum value when the electric field is considered. In the first case, it could be related to the competition between the attractive part and repulsive part of EoS. For the latter, the additional repulsive interaction can be generated by electric field and makes the minimum value shift to lower energy. In contrast to the lower beam energy case (eg., 40 MeV/nucleon), the peak value of $p_{\mathrm{T}}$ becomes larger when the Coulomb interaction is on with larger beam energy (eg., 120 MeV/nucleon), which indicates the beam energy has higher efficiency to convert into transverse energy. Furthermore,

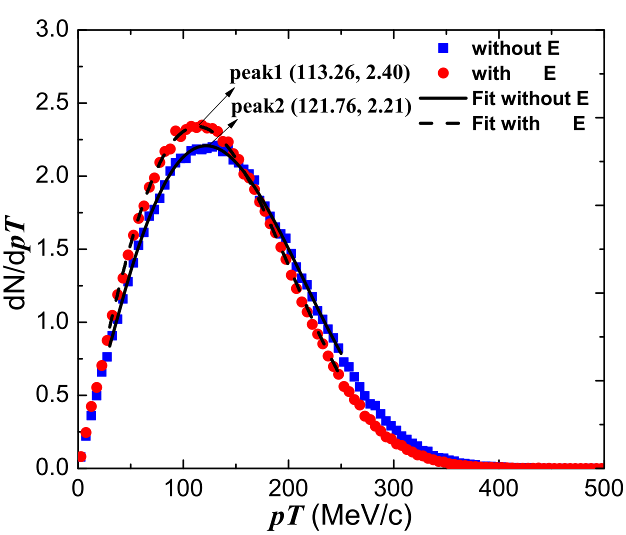


**Fig. 4** (Color online) The distribution of $p_{\mathrm{T}}$ of all nucleons at impact parameter of $b = 0$ fm for the 40 MeV/nucleon $^{208}$Pb $+^{208}$ Pb collisions

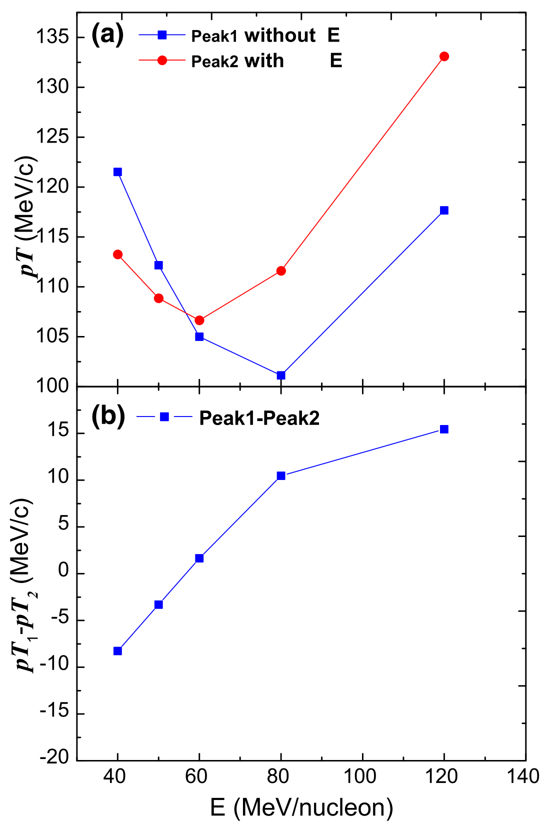


**Fig. 5** (Color online) The peak point values of $p_{\mathrm{T}}$ spectra of nucleons **a** and the change of peak point values between the cases w/ and w/o the Coulomb interaction **b** as a function of beam energies

differences of peak point values between the cases w/ and w/o Coulomb interaction increase as beam energy as shown in Fig. 5b. And the difference is vanishing around 55 MeV/nucleon. Thus, it should be paid more attention to the physics mechanism at beam energy of ranging from 40 to 80 MeV/nucleon.

To see the how electric field affects on the nucleons, the evolutions of distributions of $p_T$ of proton, neutron, and all nucleons are shown in Fig. 6. Here, we take the case without electric field as a reference. At early reaction stage of 40 fm/$c$, the protons are directly affected by the electric field as shown Fig. 6a1. And the distribution of $p_T$ is shifted to right. The shift becomes smaller as time increases. It, however, is inverse for the neutron. The difference becomes larger at the final stage. Although electric field affects on the protons directly, the neutrons are also affected during collisions. It is indicated that there is an energy transfer between the protons and neutrons.

### 3.3 Observation for magnetic effects

Pion production as an probe has been employed to investigate the magnetic effects in Ref. [9]; however, pion production energy is far from the range discussed in this paper. First, magnetic effects are considered with the distribution of $p_T$ as shown in Fig. 7. Here, the simulations include the electric field. One can see that the magnetic effects are not obvious from distribution of $p_T$. And Fig. 8 shows the ratios of neutron to proton of all and free nucleons as a function of rapidity at different impact parameters with and without magnetic field. The magnetic effects on the ratios are tiny at impact parameters of $b = 0$ fm and $b = 0.5 \times b_{\max}$ fm for 40 MeV/nucleon collisions. They are well in agreement with the results in Ref. [9].

The observables which considered in this paper basing on the momentum space of nucleons are not sensitive to the magnetic field at low energy heavy ion collisions. For the knowledge, however, the directions of charged particles can be changed by the magnetic field and fluctuations can be arisen. Thus, we consider more observables with the $z$-

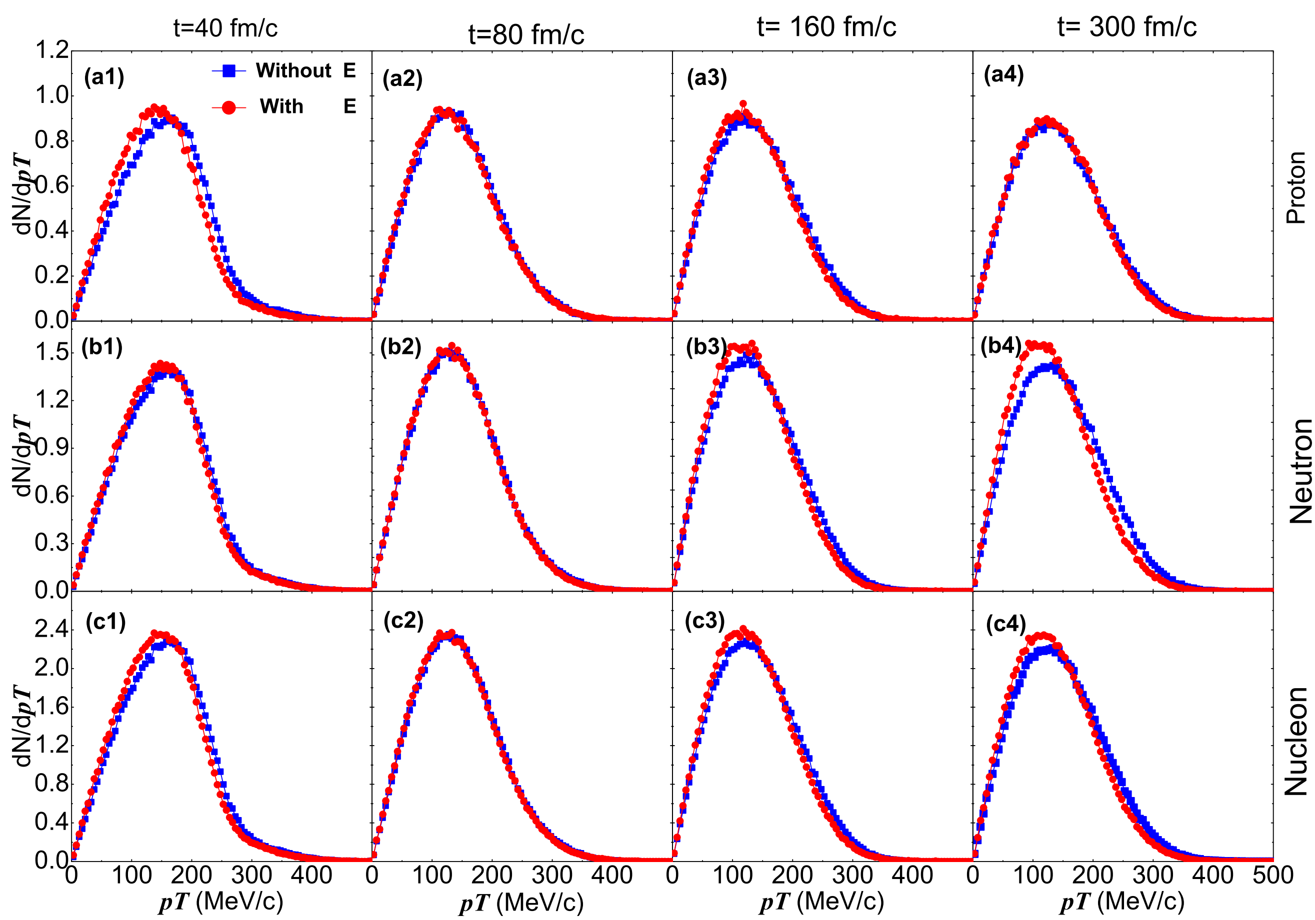


Fig. 6 (Color online) Time evolutions of distributions of $p_T$ of proton (top), neutron (middle), and all nucleons (bottom) at impact parameter of $b = 0$ fm for the 40 MeV/nucleon $^{208}$Pb $+^{208}$ Pb collisions with and without electric field

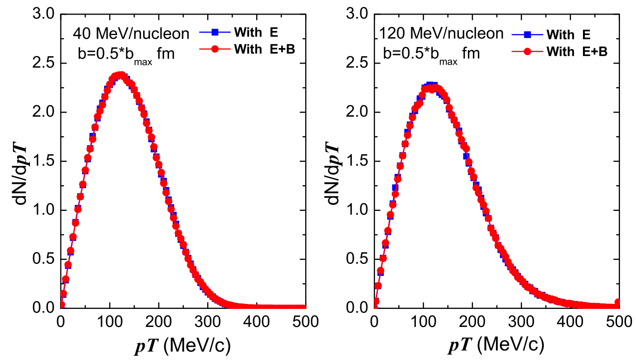


**Fig. 7** (Color online) The distribution of $p_T$ at impact parameter of $b = 0.5 \times b_{max}$ fm for 40 MeV/nucleon and 120 MeV/nucleon $^{208}$Pb $+ ^{208}$Pb collisions

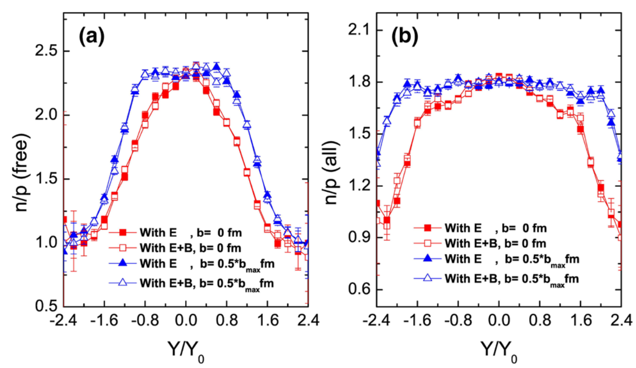


**Fig. 8** (Color online) The neutron to proton ratio of free **a** and all **b** nucleons as a function of rapidity at impact parameters of $b = 0$ fm and $b = 0.5 \times b_{max}$ fm for the 40 MeV/nucleon $^{208}$Pb $+ ^{208}$Pb collisions with and without magnetic fiel

axis direction distributions of nucleons. In Fig. 9a, the $z$-axis direction distribution of nucleons is almost symmetric in impact parameter of $b = 0$ fm. Considering the magnetic field, nucleons in the central region will be less. As beam energy increases in Fig. 9b, the difference nearly vanishes. It indicates that nucleons with high kinetic energies are not

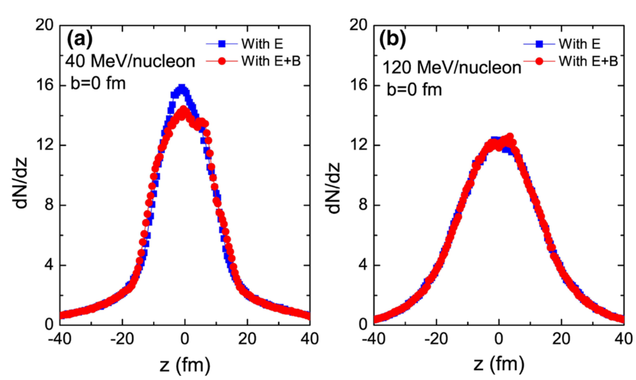


**Fig. 9** (Color online) The $z$-axis direction distributions of nucleons at impact parameters of $b = 0$ fm for 40 and 120 MeV/nucleon $^{208}$Pb $+ ^{208}$Pb collisions with and without magnetic field

nearly affected by magnetic field generated in heavy ion collisions.

## 4 Conclusion

In summary, coupling with electromagnetic field in the transport model BUU, the evolutions of electric field in the $z$ direction and magnetic field in the $y$ direction in the $x$–$z$ plane are given, and the impact parameters and incident energies dependence of the magnetic field at the center of mass are discussed. Further, we consider the electric effects from $p_T$ spectra of nucleons, two minimum values of peaks of $p_T$ spectra were found from different situations of with and without electric field. The Coulomb interaction is important for the study of heavy ion collisions. The magnetic effects are not obvious from $p_T$ spectra of nucleons, the ratio of neutron to proton of all, and free nucleons as a function of rapidity. Nevertheless, magnetic field has some effects on the $z$-axis direction distribution of nucleons.

## References

1. J. Rafelski, B. Müller, Magnetic splitting of Quasimolecular electronic states in strong fields. Phys. Rev. Lett. **36**, 517 (1976). https://doi.org/10.1103/PhysRevLett.36.517
2. K.G. Libbrecht, S.E. Koonin, Coulomb distortion of pion spectra from heavy-Ion collisions. Phys. Rev. Lett. **43**, 1581 (1979). https://doi.org/10.1103/PhysRevLett.43.1581
3. M. Gyulassy, S.K. Kauffmann, Coulomb effects in relativistic nuclear collisions. Nucl. Phys. A **362**, 503 (1981). https://doi.org/10.1016/0375-9474(81)90507-8
4. N. Auerbach, Coulomb effects in nuclear structure. Phys. Rep. **98**, 273 (1983). https://doi.org/10.1016/0370-1573(83)90008-X
5. J.J. Molitoris, J.B. Hoffer, H. Kruse et al., Microscopic calculations of collective flow probing the short-range nature of the nuclear force. Phys. Rev. Lett. **53**, 899 (1984). https://doi.org/10.1103/PhysRevLett.53.899
6. S. Pratt, Coherence and Coulomb effects on pion interferometry. Phys. Rev. D **33**, 72 (1986). https://doi.org/10.1103/PhysRevD.33.72
7. C.A. Bertulani, G. Baur, Electromagnetic processes in relativistic heavy ion collisions. Phys. Rep. **163**, 299 (1988). https://doi.org/10.1016/0370-1573(88)90142-1
8. Y.M. Zheng, C.M. Ko, B.A. Li et al., Elliptic flow in heavy-ion collisions near the balance energy. Phys. Rev. Lett. **83**, 2534 (1999). https://doi.org/10.1103/PhysRevLett.83.2534
9. L. Ou, B.A. Li, Magnetic effects in heavy-ion collisions at intermediate energies. Phys. Rev. C **84**, 064605 (2011). https://doi.org/10.1103/PhysRevC.84.064605
10. V. Skokov, A.Y. Illarionov, V. Toneev, Estimate of the magnetic field strength in heavy-ion collisions. Int. J. Mod. Phys. A **24**, 5925 (2009). https://doi.org/10.1142/S0217751X09047570
11. M. Asakawa, A. Majumder, B. Müller, Electric charge separation in strong transient magnetic fields. Phys. Rev. C **81**, 064912 (2010). https://doi.org/10.1103/PhysRevC.81.064912

12. A. Bzdak, V. Skokov, Event-by-event fluctuations of magnetic and electric fields in heavy ion collisions. Phys. Lett. B **710**, 171 (2012). https://doi.org/10.1016/j.physletb.2012.02.065
13. W.T. Deng, X.G. Huang, Event-by-event generation of electromagnetic fields in heavy-ion collisions. Phys. Rev. C **85**, 044907 (2012). https://doi.org/10.1103/PhysRevC.85.044907
14. K. Hattori, X.G. Huang, Novel quantum phenomena induced by strong magnetic fields in heavy-ion collisions. Nucl. Sci. Tech. **28**, 26 (2017). https://doi.org/10.1007/s41365-016-0178-3
15. D.E. Kharzeev, L.D. McLerran, H.J. Warringa, The effects of topological charge change in heavy ion collisions: event by event P and CP violation. Nucl. Phys. A **803**, 227 (2008). https://doi.org/10.1016/j.nuclphysa.2008.02.298
16. B.I. Abelev, M.M. Aggarwal, Z. Ahammed et al., (STAR Collaboration), Azimuthal charged-particle correlations and possible local strong parity violation. Phys. Rev. Lett. **103**, 251601 (2009). https://doi.org/10.1103/PhysRevLett.103.251601
17. B.I. Abelev, M.M. Aggarwal, Z. Ahammed et al., (STAR Collaboration), Observation of charge-dependent azimuthal correlations and possible local strong parity violation in heavy-ion collisions. Phys. Rev. C **81**, 054908 (2010). https://doi.org/10.1103/PhysRevC.81.054908
18. L. Adamczyk, J.K. Adkins, G. Agakishiev et al., (STAR Collaboration), Beam-energy dependence of charge separation along the magnetic field in $Au + Au$ collisions at RHIC. Phys. Rev. Lett. **113**, 052302 (2014). https://doi.org/10.1103/PhysRevLett.113.052302
19. L. Adamczyk, J.K. Adkins, G. Agakishiev et al., (STAR Collaboration), Observation of charge asymmetry dependence of pion elliptic flow and the possible chiral magnetic wave in heavy-ion collisions. Phys. Rev. Lett. **114**, 252302 (2015). https://doi.org/10.1103/PhysRevLett.114.252302
20. G.L. Ma, X.G. Huang, Possible observables for the chiral electric separation effect in $Cu + Au$ collisions. Phys. Rev. C **91**, 054901 (2015). https://doi.org/10.1103/PhysRevC.91.054901
21. Q.Y. Shou, G.L. Ma, Y.G. Ma, Charge separation with fluctuating domains in relativistic heavy-ion collisions. Phys. Rev. C **90**, 047901 (2014). https://doi.org/10.1103/PhysRevC.90.047901
22. C. Peng, G.X. Peng, C.J. Xia et al., Magnetized strange quark matter in the equivparticle model with both confinement and perturbative interactions. Nucl. Sci. Tech. **27**, 98 (2016). https://doi.org/10.1007/s41365-016-0095-5
23. M. Ruggieri, G.X. Peng, Chiral phase transition of quark matter in the background of parallel electric and magnetic fields. Nucl. Sci. Tech. **27**, 130 (2016). https://doi.org/10.1007/s41365-016-0139-x
24. S.S. Cui, G.X. Peng, Z.Y. Lu et al., Properties of color-flavor locked strange quark matter in an external strong magnetic field. Nucl. Sci. Tech. **26**, 040503 (2015). https://doi.org/10.13538/j.1001-8042/nst.26.040503
25. L. Adamczyk et al., (STAR Collaboration), Global $\Lambda$ hyperon polarization in nuclear collisions. Nature **548**, 62 (2017). https://doi.org/10.1038/nature23004
26. Z.T. Liang, X.N. Wang, Globally polarized quark-gluon plasma in noncentral $A + A$ collisions. Phys. Rev. Lett. **94**, 102301 (2005). https://doi.org/10.1103/PhysRevLett.94.102301
27. G.F. Bertsch, H. Kruse, S. Das, Gupta, Boltzmann equation for heavy ion collisions. Phys. Rev. C **29**, 673 (1984). https://doi.org/10.1103/PhysRevC.29.673
28. H. Kruse, B.V. Jacak, H. Stöcker, Microscopic theory of pion production and sidewards flow in heavy-ion collisions. Phys. Rev. Lett. **54**, 289 (1985). https://doi.org/10.1103/PhysRevLett.54.289
29. C.Y. Wong, H.H.K. Tang, Extended time-dependent Hartree–Fock approximation with particle collisions. Phys. Rev. Lett. **40**, 1070 (1978). https://doi.org/10.1103/PhysRevLett.40.1070
30. W. Bauer, G.F. Bertsch, W. Cassing et al., Energetic photons from intermediate energy proton-and heavy-ion-induced reactions. Phys. Rev. C **34**, 2127 (1986). https://doi.org/10.1103/PhysRevC.34.2127
31. G.F. Bertsch, S. Das, Gupta, A guide to microscopic models for intermediate energy heavy ion collisions. Phys. Rep. **160**, 189 (1988). https://doi.org/10.1016/0370-1573(88)90170-6
32. J. Cugnon, T. Mizutani, J. Vandermeulen, Equilibration in relativistic nuclear collisions. A Monte Carlo calculation. Nucl. Phys. A **352**, 505 (1981). https://doi.org/10.1016/0375-9474(81)90427-9
33. V. Voronyuk, V.D. Toneev, W. Cassing et al., Electromagnetic field evolution in relativistic heavy-ion collisions. Phys. Rev. C **83**, 054911 (2011). https://doi.org/10.1103/PhysRevC.83.054911
34. A.D. Sooda, R.K. Puri, J. Aichelin, Study of balance energy in central collisions for heavier nuclei. Phys. Lett. B **594**, 260 (2004). https://doi.org/10.1016/j.physletb.2004.05.053
35. Y.X. Zhang, Z.X. Li, Elliptic flow and system size dependence of transition energies at intermediate energies. Phys. Rev. C **74**, 014602 (2006). https://doi.org/10.1103/PhysRevC.74.014602